

# Microbioreactors for Raman Microscopy of Stromal Cell Differentiation

Vishnu Vardhan Pully,<sup>†</sup> Aufried Lenferink,<sup>†</sup> Henk-Jan van Manen,<sup>‡</sup> Vinod Subramaniam,<sup>†</sup> Clemens A. van Blitterswijk,<sup>§</sup> and Cees Otto<sup>\*,†</sup>

Biophysical Engineering Group, MIRA Institute for Biomedical Technology and Technical Medicine, MESA + Institute for Nanotechnology, University of Twente, 7522 ND Enschede, The Netherlands, Department of Analytics and Physics, Development and Innovation, AkzoNobel Research, Arnhem, The Netherlands, and Tissue Regeneration Group, MIRA Institute for Biomedical Technology and Technical Medicine, University of Twente, 7522 ND Enschede, The Netherlands

We present the development of microbioreactors with a sensitive and accurate optical coupling to a confocal Raman microspectrometer. We show that such devices enable *in situ* and *in vitro* investigation of cell cultures for tissue engineering by chemically sensitive Raman spectroscopic imaging techniques. The optical resolution of the Raman microspectrometer allows recognition and chemical analysis of subcellular features. Human bone marrow stromal cells (hBMSCs) have been followed after seeding through a phase of early proliferation until typically 21 days later, well after the cells have differentiated to osteoblasts. Long-term perfusion of cells in the dynamic culture conditions was shown to be compatible with experimental optical demands and off-line optical analysis. We show that Raman optical analysis of cells and cellular differentiation in microbioreactors is feasible down to the level of subcellular organelles during development. We conclude that microbioreactors combined with Raman microspectroscopy are a valuable tool to study hBMSC proliferation, differentiation, and development into tissues under *in situ* and *in vitro* conditions.

Cell-to-tissue development is accompanied by a combination of events such as cell proliferation, differentiation, and apoptosis. These processes are well-balanced and controlled by a number of inter- and intracellular biochemical and biophysical events. If these events are not or inappropriately performed, then cells dedifferentiate and become disorganized, a situation which may lead to cell death. *In vitro* cell-to-tissue development is usually performed either in static culture conditions using Petri dishes or tissue culture flasks, where the culture medium is refreshed periodically, or in dynamic culture conditions like bioreactors that enable continuous refreshment of the medium.<sup>1,2</sup> Bioreactors offer an advantage with respect to static conditions<sup>3,4</sup> in that biochemical

processes which take place under controlled environmental and operating conditions (such as pH, temperature, pressure, nutrient supply, and waste removal)<sup>5</sup> can be monitored in detail.

In most of the conventional static cell cultures and macroscale bioreactors, optical monitoring of nutrient supply, oxygen supply, waste removal, interaction with the extracellular matrix, and cell–cell interactions throughout the culture period is difficult. This challenge is due to the practical problem of coupling large bioreactors to noninvasive optical microscopic techniques. The advent of microfabrication technology in the field of tissue engineering has enabled new and innovative ways to analyze cellular interactions in bioreactors and cell behavior in a microfluidic environment that mimic *in vivo* body conditions.<sup>6,7</sup> The microfluidic bioreactors or microbioreactors are microscale versions of conventional bioreactors with significant advantages in terms of cost-effectiveness, portability, performance, and materials used. The implementation of microbioreactors offers a suitable environment for various cell- and tissue-based applications as has been widely demonstrated.<sup>8,9</sup> An overview is shown in Table 1.<sup>10–17</sup>

Monitoring of cellular organelles and development of cells to tissues over a longer period of time is most frequently performed

\* To whom correspondence should be addressed. Phone: +31 53 4893159. Fax: +31 53 4891105. E-mail: c.otto@utwente.nl.

<sup>†</sup> Biophysical Engineering Group, University of Twente.

<sup>‡</sup> AkzoNobel Research.

<sup>§</sup> Tissue Regeneration Group, University of Twente.

(1) Dexter, T. M.; Allen, T. D.; Lajtha, L. G.; Schofield, R.; Lord, B. I. *J. Cell. Physiol.* **1973**, *82*, 461–473.

(2) Langer, R.; Vacanti, J. P. *Science* **1993**, *260*, 920–926.

(3) Cabral, J. M. S. *Biotechnol. Lett.* **2001**, *23*, 741–751.

(4) Collins, P. C.; Miller, W. M.; Papoutsakis, E. T. *Biotechnol. Bioeng.* **1998**, *59*, 534–543.

(5) Martin, I.; Wendt, D.; Heberer, M. *Trends Biotechnol.* **2004**, *22*, 80–86.

(6) Griffiths, L. A.; Naughton, G. *Science* **2002**, *295*, 1009–1014.

(7) Strain, A. L.; Neuberger, J.; Neuberger, J. M. *Science* **2002**, *295*, 1005–1009.

(8) Andersson, H.; van den Berg, A. *Sens. Actuators, B* **2003**, *B92*, 315–325.

(9) Palkova, Z.; Vachova, L.; Valer, M.; Preckel, T. *Cytometry, Part A* **2004**, *59*, 246–253.

(10) Borenstein, J. T.; Terai, H.; King, K. R.; Weinberg, E. J.; Kaazempur-Mofrad, M. R.; Vacanti, J. P. *Biomed. Microdevices* **2002**, *4*, 167–175.

(11) Chang, W.-J.; Akin, D.; Sedlak, M.; Ladisch, M. R.; Bashir, R. *Biomed. Microdevices* **2003**, *5*, 281–290.

(12) Leclerc, E.; David, B.; Griscorn, L.; Lepioufle, B.; Fujii, T.; Layrolle, P.; Legallais, C. *Biomaterials* **2006**, *27*, 586–595.

(13) Petersen, E. F.; Spencer, R. G. S.; McFarland, E. W. *Biotechnol. Bioeng.* **2002**, *78*, 801–804.

(14) Pins, G. D.; Toner, M.; Morgan, J. R. *FASEB J.* **2000**, *14*, 593–602.

(15) Powers, M. J.; Domansky, K.; Kaazempur-Mofrad, M. R.; Kalezi, A.; Capitano, A.; Upadhyaya, A.; Kurzawski, P.; Wack, K. E.; Stolz, D. B.; Kamm, R.; Griffith, L. G. *Biotechnol. Bioeng.* **2002**, *78*, 257–269.

(16) Taylor, A. M.; Rhee, S. W.; Tu, C. H.; Cribbs, D. H.; Cotman, C. W.; Jeon, N. L. *Langmuir* **2003**, *19*, 1551–1556.

(17) Wheeler, A. R.; Thordset, W. R.; Whelan, R. J.; Leach, A. M.; Zare, R. N.; Liao, Y. H.; Farrell, K.; Manger, I. D.; Daridon, A. *Anal. Chem.* **2003**, *75*, 3581–3586.

**Table 1. Microbioreactors for Cell and Tissue Applications**

microbioreactor type	application	ref
poly(dimethylsiloxane) (PDMS) microfabricated array bioreactor	three-dimensional liver cultures	15
PDMS layers sealed to positive and negative silicon micromachined mold wafers	vascularized tissue using endothelial cells	10
multilayered PDMS microfluidic device	analysis of single cells	17
PDMS and silicon hybrid biochip	culture of <i>Listeria innocua</i> and <i>Escherichia coli</i> bacteria	11
3D PDMS microbioreactor	bone tissue engineering using mouse calvarial osteoblastic cells	12
PDMS membranes resembling basal lamina laminated to collagen type I sponges	culturing human epidermal keratinocytes to form a skin equivalent	14
micropatterned flexible biocompatible polysaccharide gel	culturing chondrocytes for reparative cartilage in vitro	13
PDMS and glass biochip	nerve cell culture	16

by fluorescence microscopy.<sup>18</sup> However, it is quite common that the fluorescent dyes used for specific subcellular staining interfere with the development of cells and tissues. The hydrophobicity of fluorescent stains may also cause them to adhere to glass or polymers, which are used for the fabrication of the microbioreactors. These aspects make fluorescence staining strategies less desirable.<sup>19</sup> Since the first application of Raman microspectroscopy to cells,<sup>20</sup> this technique has been widely used for biological applications. Raman microspectroscopy provides chemical information from cells or tissues in a noninvasive and label-free way. Applications of Raman spectroscopy of cells has demonstrated that it is able to determine cellular status, such as living cells,<sup>20,21</sup> dead cells,<sup>22</sup> apoptotic cells,<sup>23</sup> cells in mitotic stage,<sup>24</sup> proliferating cells,<sup>25</sup> and differentiating cells.<sup>26</sup> Recently, Raman spectroscopy has been extended to obtain chemical information over extended periods of time from cells cultured in a microfluidic environment.<sup>27–31</sup> The combination of optical tweezers and a microfluidic system to trap single red blood cells for Raman measurements was successfully shown.<sup>29,30</sup> Surface-enhanced Raman spectroscopy (SERS) using gold nanoparticles for Raman enhancement was used to study the real-time spectral response from a single living Chinese hamster ovary cell in a microfluidic system.<sup>31</sup> Identification of

different bacteria by SERS was shown on a microfluidic platform over a single chip.<sup>27</sup> The combination of SERS with microfluidics and its application to molecular and cellular analysis has recently been reviewed.<sup>28</sup>

In this paper we show two types of microbioreactors for cell- and tissue-based applications. The first microbioreactor ( $\mu$ BR-I), based on poly(dimethylsiloxane) (PDMS) technology in combination with a calcium fluoride ( $\text{CaF}_2$ ) substrate, was used to study the human bone marrow stromal cells (hBMSCs) proliferation and differentiation toward mineralized tissue over a 21 day culture period. The second microbioreactor ( $\mu$ BR-II), made from a combination of a commercially available ibidi  $\mu$ -slide 1 luer (ibidi GmbH, München, Germany) and a glass coverslip, enabled chemical imaging of cells cultured over a 10 day time period. Throughout the entire culture period, normal cell development and growth rates were observed in the microbioreactors, which were continuously perfused with cell culture medium. Biochemical processes in hBMSCs in both types of microbioreactors were successfully monitored by confocal Raman microspectroscopy without causing any damage to the cells. Raman results from the  $\mu$ BR-I showed hBMSC proliferation, differentiation, and mineralization over the culture period. Chemical mapping of single hBMSCs cultured in  $\mu$ BR-II showed distributions of organelles in individual cells.

## MATERIALS AND METHODS

**Microbioreactor Design.** Although many types of microbioreactors have been reported in the literature (Table 1), the motivation behind the design of our microbioreactors  $\mu$ BR-I and  $\mu$ BR-II are to enable confocal Raman microspectroscopy to monitor cell proliferation, differentiation, and other intracellular processes inside the microbioreactor. Most bioreactors presented in the literature are fabricated using polymers. The strong Raman scattering of organic polymers, particularly in comparison with the weak Raman scattering from subcellular volumes, requires a careful design of the microbioreactor. We have chosen a combination of a polymer and optically silent materials such as  $\text{CaF}_2$  and glass coverslip (borosilicate glass) for the design of microbioreactors. The  $\mu$ BR-I was fabricated from PDMS and a  $\text{CaF}_2$  substrate (Crystran Ltd., Poole, U.K.), as shown in Figure 1, parts A and B. The PDMS chip utilizes microfabrication technology which includes photolithography and replica molding. These

- (18) Olson, K. J.; Ahmadzadeh, H.; Arriaga, E. A. *Anal. Bioanal. Chem.* **2005**, *382*, 906–917.
- (19) Piruska, A.; Nikcevic, I.; Lee, S. H.; Ahn, C.; Heineman, W. R.; Limbach, P. A.; Seliskar, C. J. *Lab Chip* **2005**, *5*, 1348–1354.
- (20) Puppels, G. J.; De Mul, F. F. M.; Otto, C.; Greve, J.; Robert-Nicoud, M.; Arndt-Jovin, D. J.; Jovin, T. M. *Nature* **1990**, *347*, 301–303.
- (21) Nottingher, I.; Verrier, S.; Romanska, H.; Bishop, A. E.; Polak, J. M.; Hench, L. L. *Spectroscopy* **2002**, *16*, 43–51.
- (22) Verrier, S.; Nottingher, I.; Polak, J. M.; Hench, L. L. *Biopolymers* **2004**, *74*, 157–162.
- (23) Uzunbajakava, N.; Lenferink, A.; Kraan, Y.; Volokhina, E.; Vrensen, G.; Greve, J.; Otto, C. *Biophys. J.* **2003**, *84*, 3968–3981.
- (24) Matthaues, C.; Boydston-White, S.; Miljkovic, M.; Romeo, M.; Diem, M. *Appl. Spectrosc.* **2006**, *60*, 1–8.
- (25) Short, K. W.; Carpenter, S.; Freyer, J. P.; Maurant, J. R. *Biophys. J.* **2005**, *88*, 4274–4288.
- (26) Nottingher, I.; Jell, G.; Lohbauer, U.; Salih, V.; Hench, L. L. *J. Cell. Biochem.* **2004**, *92*, 1180–1192.
- (27) Cheng, I. F.; Chang, H.-C.; Hou, D.; Chang, H.-C. *Biomicrofluidics* **2007**, *1*, 21503.
- (28) Huh, Y. S.; Chung, A. J.; Erickson, D. *Microfluid. Nanofluid.* **2009**, *6*, 285–297.
- (29) Ramser, K.; Enger, J.; Goksoer, M.; Hanstorp, D.; Logg, K.; Kaell, M. *Lab Chip* **2005**, *5*, 431–436.
- (30) Ramser, K.; Wenseleers, W.; Dewilde, S.; Van Doorslaer, S.; Moens, L. *Spectroscopy* **2008**, *22*, 287–295.
- (31) Zhang, X.; Yin, H.; Cooper, J. M.; Haswell, S. J. *Anal. Bioanal. Chem.* **2008**, *390*, 833–840.

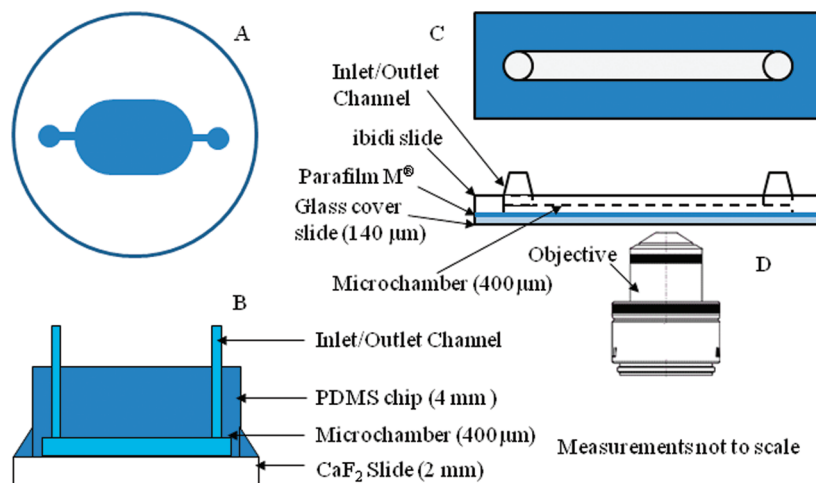


**Figure 1.** Microbioreactors for cell- and tissue-based applications enabling noninvasive and label-free Raman measurements: (A) top view of BR-I, (B) cross-sectional view of  $\mu$ BR-I, (C) top view of  $\mu$ BR-II, and (D) cross-sectional view of  $\mu$ BR-II showing the feasibility of optical measurements through the glass coverslide.

steps have been extensively described in the literature.<sup>12,32,33</sup> The fabricated PDMS chip has a diameter of 25 mm and a thickness of 4 mm. The PDMS chip has a microchamber (12 mm (length)  $\times$  8 mm (breadth)  $\times$  400  $\mu$ m (height)) for cell culture and two microchannels, input and output, for nutrient supply and waste removal. The microbioreactor is closed and sealed by laying the PDMS chip over the  $\text{CaF}_2$  substrate (circular discs with 35 mm diameter and 2 mm thickness).  $\text{CaF}_2$  forms the substrate for the cells in the microbioreactor. We have never observed any effect of  $\text{CaF}_2$  on the development of cells. The semicircular sides of the microchamber in  $\mu$ BR-I (Figure 1A) form a hydrodynamic structure that enables a good flow profile for medium perfusion through the microbioreactor, which results in the removal of air bubbles from the microchamber or microchannels and enables effective nourishment of the cultured cells.  $\mu$ BR-II was fabricated from a bottomless  $\mu$ -slide 1 luer (ibidi GmbH, München, Germany) with provisions for an inlet and outlet channel and a glass coverslip (thickness  $\sim$ 140  $\mu$ m) (Menzel Gläser, Braunschweig, Germany) sealed to the bottom with Parafilm M (Pechiney Plastic Packaging, Illinois). A secure bonding between the ibidi  $\mu$ -slide 1 luer and the glass coverslip was achieved by heating the Parafilm M to around 65  $^{\circ}\text{C}$ . Sealing created a well-defined microchamber (50 mm (length)  $\times$  5 mm (breadth)  $\times$  400  $\mu$ m (height)) where hBMSCs were cultured and where perfusion of the cells with a culture medium was feasible. Silicon tubes (Pharmed BPT, Materflex, Cole-Palmer, Illinois) connected the inlet and outlet of the microbioreactors to the peristaltic pump via luer adaptors. The procedure for building these microbioreactors yielded tight bonds between the PDMS chip and  $\text{CaF}_2$  substrate in  $\mu$ BR-I and ibidi  $\mu$ -slide 1 luer and glass coverslide in  $\mu$ BR-II. These bonds are sufficiently strong to withstand the flow rates used during long-term cell culture.

**Sterilization of the Perfusion System.** The perfusion circuit was realized by fixing the microbioreactors, silicon tubing, a peristaltic pump (Peri-Star PR, World Precision instruments, Florida), and the culture medium flasks in a closed loop. The

perfusion circuit was sterilized by perfusing 70% ethanol through the circuit and subsequently autoclaving the entire system for 35 min. Poly-L-lysine solution is perfused into  $\mu$ BR-I and  $\mu$ BR-II in order to coat the inner surfaces of the microchamber, while residing in an incubator for about 40 min at 37  $^{\circ}\text{C}$  in an atmosphere with 95% humidity and 5% partial pressure of  $\text{CO}_2$ . A poly-L-lysine coating enhances stable cell adhesion on the walls of the microchamber in the microbioreactor. The perfusion circuit was then perfused with Dulbecco's phosphate-buffered saline (PBS) to remove any excess poly-L-lysine solution.

**Cell Culture.** hBMSCs from bone marrow aspirates of healthy human donors were seeded at cell densities of 5000 cells/ $\text{cm}^2$  and cultured overnight in basic medium to allow cell adhesion on the  $\text{CaF}_2$  substrate or glass coverslide of the respective microbioreactors. Basic medium (BM), which was taken as a control condition, was prepared from  $\alpha$ -minimum essential medium ( $\alpha$ -MEM; Gibco, Carlsbad, CA), 10% fetal bovine serum (FBS; Bio Whittaker, Australia), 0.2 mM L-ascorbic acid-2-phosphate (Asap; Sigma, St. Louis, MO), 100 U/mL penicillin G (Invitrogen, Carlsbad, CA), 100  $\mu\text{g}/\text{mL}$  streptomycin (Invitrogen), and 2 mM L-glutamine (L-glu; Sigma). After overnight culture in BM, osteogenic culture medium was continuously perfused with a flow rate of 10  $\mu\text{L}/\text{min}$  to establish a dynamic culture system. Osteogenic mineralization medium (OM) was prepared by adding 0.01 M  $\beta$ -glycerophosphate ( $\beta$ GP; Sigma) and  $10^{-8}$  M dexamethasone (Dex; Sigma) to BM.<sup>34</sup> Throughout the culture period, the entire system was placed in an incubator maintained at 37  $^{\circ}\text{C}$  in an atmosphere with 95% humidity and 5% partial pressure of  $\text{CO}_2$ . The stock solution of the culture medium was changed every 2 days during the culture period to supply sufficient nutrients to the cells. Confocal Raman measurements were performed on cells cultured in  $\mu$ BR-I after day 1, day 14, and day 21 of the culture period and on day 4 of the culture period for  $\mu$ BR-II. On each measurement day, the microbioreactors with cells cultured in them were washed thrice with phosphate-buffered saline solution (PBS; Gibco) before being transferred to the confocal Raman microscopy for

(32) Enger, J.; Goksoer, M.; Ramser, K.; Hagberg, P.; Hanstorp, D. *Lab Chip* **2004**, *4*, 196–200.

(33) Leclerc, E.; Sakai, Y.; Fujii, T. *Biotechnol. Prog.* **2004**, *20*, 750–755.

(34) Bellows, C. G.; Heersche, J. N. M.; Aubin, J. E. *Dev. Biol.* **1990**, *140*, 132–138.



measurements on living cells. After the measurements  $\mu$ BR-II was placed into the incubator after exchanging the PBS buffer for the nutrient medium and connecting it to the continuous perfusion system for further culture.

**Confocal Raman Microscopy.** Raman measurements on hBMSCs were performed using a custom-built confocal Raman spectrometer. A Kr-ion laser (Coherent, Innova 90-K, Santa Clara, CA) with an emission wavelength of 647.1 nm was used as an excitation source. Raman spectra from the cells cultured in  $\mu$ BR-I were acquired using a 63 $\times$ /1.2 NA water-immersion objective (Plan Neofluar; Carl Zeiss, Jena, Germany). The scattered light is collected in epi-detection mode, filtered by a razor-edge filter (Semrock, Rochester, NY) to suppress reflected laser light and Rayleigh scattered light, and focused onto a pinhole (25  $\mu$ m diameter) at the entrance of an imaging spectrograph/monochromator (HR460; Jobin-Yvon, Paris, France), which contains a blazed holographic grating with 600 grooves/mm. A thermoelectrically cooled CCD detector containing a back-illuminated chip with 1340  $\times$  100 pixels of 20  $\times$  20  $\mu$ m<sup>2</sup> (PIXIS 100, Princeton Instruments, NJ) is placed in the focal plane of the spectrograph exit port. The spectrograph/camera combination provides a spectral resolution of 2.10 cm<sup>-1</sup>/pixel on average over the Raman spectral range from 300 to 2000 cm<sup>-1</sup>. To obtain the Raman spectra of cells in the  $\mu$ BR-II, a coverslip-corrected water-immersion objective 63 $\times$ /1.2 NA (Plan Neofluar; Carl Zeiss, Jena, Germany) was used.

Raman measurements of hBMSC cells in  $\mu$ BR-I were acquired in so-called "spectral scanning mode" on each measurement day after peeling off the PDMS layer from the CaF<sub>2</sub> substrate. The CaF<sub>2</sub> substrate with live cells was placed in a Petri dish containing PBS buffer and measured with a 63 $\times$  water-immersion objective. In "spectral scanning mode" a single full spectrum is obtained by raster-scanning the laser beam over an area of 15  $\times$  15  $\mu$ m<sup>2</sup> in 60 s with a laser power of 75 mW. This procedure results in a relatively low light dose of 2 mJ/ $\mu$ m<sup>2</sup>. Raman spectra were acquired from 10 randomly chosen cells in each culture medium for day 1, day 14, and day 21 of the culture period. Live-cell Raman imaging of hBMSCs cultured in  $\mu$ BR-II until day 4 of the culture period was performed in situ inside the microbio reactor (Figure 1D). Raman images were acquired over an area of 15  $\times$  15  $\mu$ m<sup>2</sup> with a pixel size of 468 nm, an accumulation time of 0.5 s per pixel, and an excitation power of 50 mW.

**Raman Data Analysis.** The preprocessing of the data was performed as described in the literature.<sup>23,35–37</sup> The Raman spectra were preprocessed by subtraction of the camera offset and calibration of the wavenumber axis. The well-known band positions of toluene were used to relate wavenumbers to pixels. The hyperspectral data cube obtained in Raman imaging is subjected to singular value decomposition (SVD) to improve the signal-to-noise ratio.<sup>23,35–37</sup> After data preprocessing, all 10 spectra from individual cells on respective measurement days from  $\mu$ BR-I were averaged and normalized to the mean. The data acquired

from  $\mu$ BR-II were preprocessed and treated with hierarchical cluster analysis (HCA), a multivariate data analysis technique.<sup>38</sup> HCA was performed over the spectral range of 500–1800 cm<sup>-1</sup>. All data manipulations were performed with routines written in MATLAB 7.4 (The Math Works Inc., Natick, MA).

## RESULTS AND DISCUSSION

Most bioreactors described in the literature (Table 1) are fabricated with PDMS technology and sometimes in combination with glass. This robust and flexible technology was also used for  $\mu$ BR-I. Elastomeric materials such as PDMS are widely used for soft lithography of microbio reactor fabrication. PDMS is optically transparent down to UV ranges of about 280 nm.<sup>39</sup> The material is cost-effective and offers good mechanical flexibility. Furthermore, it is biocompatible with biological assays and cells and permeable to oxygen that is sufficient for cells.<sup>40–42</sup> Figure 1 shows the microbio reactors that we designed for long-term perfusion culture of cells. Parts A and B of Figure 1 show the top and the cross-sectional view of the  $\mu$ BR-I. The upper part is made of PDMS and has a well-defined microchamber for cell culture and input and output microchannels for nutrient supply. A CaF<sub>2</sub> substrate forms the lower part of the microbio reactor. The hBMSCs are cultured on CaF<sub>2</sub> substrate. CaF<sub>2</sub> is optically transparent and is well-known for a low contribution to background in Raman spectra. We have never observed an adverse effect of CaF<sub>2</sub> on our cell cultures. The  $\mu$ BR-I provided a working volume of 34.5  $\mu$ L and a surface area of 86.26 mm<sup>2</sup> where the cells were cultured. The top and cross-sectional views of  $\mu$ BR-II are shown in Figure 1, parts C and D, respectively. The choice of materials was guided by optical transparency and biocompatibility with long-term perfusion culture of cells. The Parafilm M provided a good bonding between the "ibidi  $\mu$ -slide 1 luer" and a glass coverslip throughout the culture period. As a proof of concept, HeLa cells were successfully cultured under dynamic culture conditions in  $\mu$ BR-II for a period of 10 days with Raman spectroscopic imaging being performed every 3 days (Supporting Information Figures S1 and S2). Normal cell growth and proliferation occurred over the culture period, reflecting the feasibility of the  $\mu$ BR-II for long-term cell cultures.  $\mu$ BR-II has a working volume of 100  $\mu$ L and a cell culture surface area of 250 mm<sup>2</sup> over the glass coverslip. The microchannels for the supply of the nutrients are prepared from silicon tubes. Both  $\mu$ BR-I and  $\mu$ BR-II microbio reactors enabled successful cell culture under long-term perfusion with a uniform laminar flow of the nutrient medium through the microchamber.

For Raman studies of cells, the choice of substrate used for cell culture is of paramount importance. Figure 2 compares the Raman spectra of cells with those of different candidate materials for bioreactors. The Raman spectrum from CaF<sub>2</sub> has a single strong vibration at 320 cm<sup>-1</sup> and none in the chosen region as seen in Figure 2, curve i. The spectrum of PDMS in Figure 2, curve vi, shows intense bands over the fingerprint region. The

(35) Pully, V. V.; Lenferink, A.; Otto, C. J. *Raman Spectrosc.* [Online early access]. DOI: 10.1002/jrs.2501. Published Online: Oct 12, 2009. <http://www3.interscience.wiley.com/journal/122626094/abstract>.

(36) Uzunbajakava, N.; Greve, J.; Otto, C. *Proc. SPIE—Int. Soc. Opt. Eng.* **2003**, 4963, 223–230.

(37) Van Manen, H.-J.; Kraan, Y. M.; Roos, D.; Otto, C. J. *Phys. Chem. B* **2004**, 108, 18762–18771.

(38) van Manen, H.-J.; Kraan, Y. M.; Roos, D.; Otto, C. *Proc. Natl. Acad. Sci. U.S.A.* **2005**, 102, 10159–10164.

(39) McDonald, J. C.; Duffy, D. C.; Anderson, J. R.; Chiu, D. T.; Wu, H.; Schueller, O. J.; Whitesides, G. M. *Electrophoresis* **2000**, 21, 27–40.

(40) Charati, S. G.; Stern, S. A. *Macromolecules* **1998**, 31, 5529–5535.

(41) El-Ali, J.; Sorger, P. K.; Jensen, K. F. *Nature* **2006**, 442, 403–411.

(42) Leclerc, E.; Sakai, Y.; Fujii, T. *Biomed. Microdevices* **2003**, 5, 109–114.

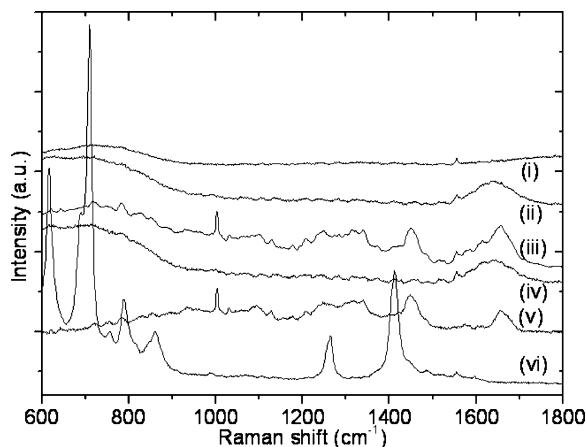


**Figure 2.** Comparison of Raman spectra of cells with those of different candidate materials for bioreactors: (i)  $\text{CaF}_2$  substrate, (ii) PBS solution, (iii) average spectra from randomly chosen 10 individual hBMSCs, (iv) average of 10 spectra obtained from the same height next to the hBMSCs, (v) Raman difference spectrum of spectrum iii minus spectrum iv showing the background-free cell spectrum, and (vi) PDMS polymer. Each spectrum is obtained by spectral scanning over an area  $15 \times 15 \mu\text{m}^2$  with an accumulation time of 60 s and 75 mW of laser power.

Raman spectrum from the PBS solution has a broad band around  $1540\text{--}1760 \text{ cm}^{-1}$  corresponding to the OH bending vibration of water (Figure 2, curve ii). The average of 10 individual hBMSC spectra, shown in Figure 2, curve iii, features prominent bands for nucleotides, amides, and proteins.<sup>43–45</sup> The spectrum in Figure 2, curve iv, is obtained from the average of 10 individual spectra obtained from the same focusing height adjacent to the cells on the  $\text{CaF}_2$  substrate and is similar to the PBS spectrum shown in Figure 2, curve ii. The Raman difference spectrum of the average of hBMSCs minus the average spectra obtained adjacent to the corresponding cell is shown in Figure 2, curve v. The difference spectrum shows prominent bands for nucleotides, amides, and proteins<sup>43–45</sup> which are free from the spectral influences of  $\text{CaF}_2$  and PBS. The PDMS spectrum shows bands (Figure 2, curve vi) which overlap with bands from hBMSCs as seen in Figure 2, curve iii. Due to the high Raman scattering of PDMS in the fingerprint region,  $\text{CaF}_2$  is a better substrate for Raman studies of cell cultures in microbioreactors. All other spectra show a broad spectral response around  $600\text{--}900 \text{ cm}^{-1}$  from water and a band at  $1555 \text{ cm}^{-1}$  which is due to oxygen in the optical beamline. These features are not observed in the Raman difference spectrum in Figure 2, curve v.

The  $\mu\text{BR-I}$  and  $\mu\text{BR-II}$  operate under laminar flow conditions. A flow rate of around  $10 \mu\text{L}/\text{min}$  was maintained throughout the culture period, providing enough nutrients to the cells without detaching them from the surface of respective substrate by flow-force. Due to the continuous supply of the nutrient medium, no  $\text{CO}_2$  buffering was required to maintain the pH. As the PDMS and silicon tubes are permeable to  $\text{O}_2$ , the cells acquired sufficient  $\text{O}_2$  throughout the culture period.<sup>46</sup> Flow rates larger

than  $20 \mu\text{L}/\text{min}$  resulted in detachment of cells from the surface of the microchamber. The hBMSCs successfully proliferated in the microbioreactors after sterilization and surface treatment as described in the Materials and Methods. The hBMSCs were well-preserved in perfusion culture until day 21 of the culture period, indicating that a sufficient supply of nutrients, oxygen, and an efficient removal of waste was achieved by the action of the peristaltic pump. The experiments show that long-term culture of cells in microbioreactors under well-maintained conditions is feasible.

Confocal Raman microscopy of cells results in chemical information by a label-free and noninvasive method. Raman microspectroscopy as a function of time of hBMSCs cultured in the  $\mu\text{BR-I}$  was obtained from measurements in separate microbioreactors with different culture media conditions. hBMSCs were cultured in both basic medium and osteogenic medium until day 1, day 14, and day 21 of the culture period, respectively. Monitoring cell development in a single microbioreactor over the entire culture period was not feasible with  $\mu\text{BR-I}$ . This is due to the relatively thick top layer of PDMS and the intense Raman scattering of this material throughout the fingerprint region Figure 2. Observation of the cells through the bottom layer of the  $\text{CaF}_2$  is possible; however, the optical quality of the focus is low due to aberration caused by the thickness of the  $\text{CaF}_2$  substrate and the accompanying large refractive index mismatch. Hence, the PDMS chip was peeled off from the  $\text{CaF}_2$  substrate to accommodate the Raman measurements on the cultured hBMSCs. The average Raman spectra from cells in respective culture media condition are shown in Figure 3 for each measurement day.

hBMSCs were cultured in parallel in separate  $\mu\text{BR-I}$ . On each measurement day, 10 hBMSCs from a single microbioreactor were randomly selected. The Raman spectra from all 10 hBMSC were averaged. The average Raman spectrum of hBMSCs cultured overnight in BM (day 1) is shown in Figure 3A, curve i. It shows Raman bands originating from the presence of biomolecules such as DNA at  $788 \text{ cm}^{-1}$ , phenylalanine at  $1004$  and  $1032 \text{ cm}^{-1}$ , nucleotide backbone at  $1094 \text{ cm}^{-1}$ , protein at  $1126 \text{ cm}^{-1}$ , adenine at  $1304$  and  $1339 \text{ cm}^{-1}$ , and a broad amide-I band at  $1660 \text{ cm}^{-1}$ .<sup>43–45</sup> Average Raman spectra from hBMSCs cultured in basic medium until day 14 and day 21 are shown in Figure 3A, curves ii and iii. These spectra show bands at similar positions as those seen after overnight culture in Figure 3A, curve i. The spectra in Figure 3A are not significantly different, which can be expected since the basic medium maintains a normal growth of cells throughout the culture period. In order to differentiate the hBMSCs toward the osteogenic lineage, another set of  $\mu\text{BR-I}$  was used, which were perfused with osteogenic media after the overnight culture period. The spectral response, due to the influence of osteogenic media on the hBMSCs cultured until day 14 and day 21 of culture period, are shown in Figure 3B, curves i and ii, respectively, over the spectral region of  $800\text{--}1200 \text{ cm}^{-1}$ . The presence of Dex in the osteogenic media induced osteogenic differentiation of hBMSCs, whereas the presence of  $\beta\text{GP}$  results in mineralization of the hBMSCs within the culture period. Both spectra in Figure 3B, curves i and ii, show a prominent band around  $961 \text{ cm}^{-1}$  reflecting the presence of the

(43) Hayashi, H.; Nishimura, Y.; Katahira, M.; Tsuboi, M. *Nucleic Acids Res.* **1986**, *14*, 2583–2596.

(44) Thomas, G. J., Jr.; Prescott, B.; Olins, D. E. *Science* **1977**, *197*, 385–388.

(45) Tu, A. T. *Raman Spectroscopy in Biology: Principles and Applications*, 1982.

(46) Hung Paul, J.; Lee Philip, J.; Sabounchi, P.; Lin, R.; Lee Luke, P. *Biotechnol. Bioeng.* **2005**, *89*, 1–8.

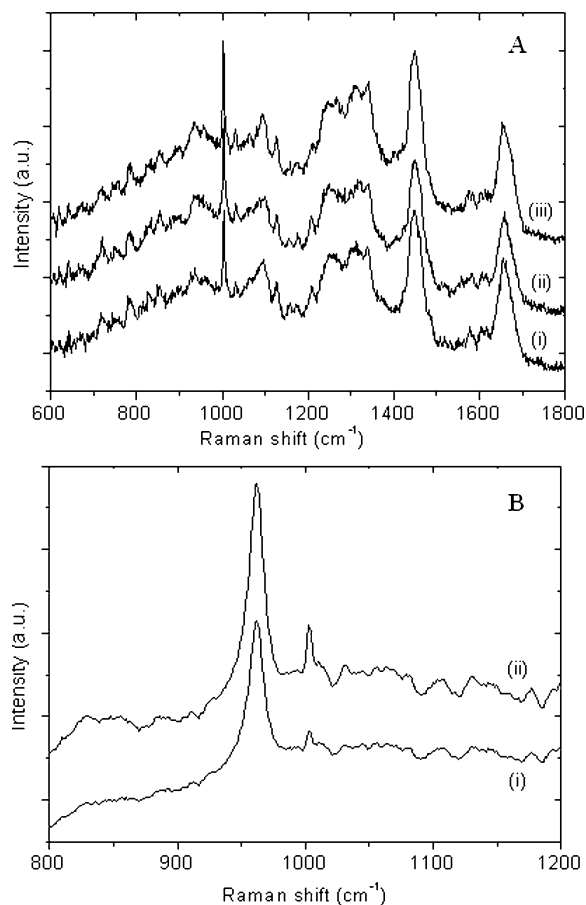


**Figure 3.** Raman microspectroscopy of hBMSCs cultured in  $\mu$ BR-I over a 21 day culture period under the influence of continuous perfusion of culture medium: (A) average of 10 spectra from hBMSCs cultured in basic medium up to (i) day 1, (ii) day 14, and (iii) day 21 of the culture period; (B) average of 10 spectra from hBMSCs cultured in osteogenic medium up to (i) day 14 and (ii) day 21 of the culture period showing mineralization over the cells. Each spectrum is obtained by spectral scanning over an area of  $15 \times 15 \mu\text{m}^2$  with an accumulation time of 60 s and 75 mW of laser power.

$\nu_1$  vibration of phosphates.<sup>47,48</sup> The position of the band corresponds to phosphates in hydroxyapatite minerals, which are part of the extracellular matrix of the hBMSCs. The increase in intensity of the phosphate band on day 21 compared to day 14 signifies the growth of the formed hydroxyapatite. Each of the average spectra in Figure 3, parts A and B, are corrected for the influence of PBS buffer. Our results show the feasibility of the  $\mu$ BR-I for long-term perfusion culture to study the proliferation, differentiation, and mineralization of hBMSCs. Raman difference spectra of average spectra obtained on day 14 and day 21 with respect to day 1 did not show prominent bands around 1578 and 1607  $\text{cm}^{-1}$ , which have been proposed<sup>21</sup> as biomarkers for necrotic cells. This observation suggests that the hBMSCs were maintained in healthy metabolic conditions up to day 21 of the culture period,<sup>21</sup> without any significant occurrence of cell death due to apoptosis and necrosis.

A limitation of  $\mu$ BR-I is that the PDMS layer had to be peeled off the  $\text{CaF}_2$  substrate. In order to overcome this limitation we developed  $\mu$ BR-II, which enabled Raman imaging of the hBMSCs over the culture period through the glass coverslip with a standard microscope and a coverglass-corrected microscope objective as shown in Figure 1D. The hBMSCs were successfully cultured in these microbioreactors under the influence of basic media up to day 4 of the culture period. Live-cell Raman imaging of the hBMSC was performed by scanning in  $32 \times 32$  steps in an area of  $15 \times 15 \mu\text{m}^2$  with an accumulation time of 0.5 s per pixel and 50 mW of laser power. Figure 4A shows the white-light micrograph of a hBMSC with a  $15 \times 15 \mu\text{m}^2$  white frame showing the region of interest for Raman imaging. The corresponding two-cluster HCA image after cluster analysis over the 500–1850  $\text{cm}^{-1}$  is shown in Figure 4B, and the respective average spectra of each cluster are shown in Figure 4D over the spectral region of 600–1800  $\text{cm}^{-1}$ . In Figure 4B, one cluster (black pixels) corresponds to the cell and the other cluster corresponds to the background (PBS buffer) (magenta pixels). The spectra corresponding to the respective clusters are shown in Figure 4D, curves i and ii. The average background spectrum is influenced by contributions from the glass substrate (855–955  $\text{cm}^{-1}$ ) and PBS buffer. The cell spectrum shows prominent bands reflecting the presence of nucleotides, proteins, and lipids. The background-free cell spectrum is obtained by subtracting the background spectrum from the cell spectrum, as shown in Figure 4D, curve iii. The resultant spectrum is free from the contributions of glass and PBS buffer, has a baseline close to zero, and reveals many pronounced vibrational bands, which can be assigned to nucleotides, proteins, and lipids in agreement with the literature.<sup>43–45</sup>

The cell spectra in Figure 4D, curves i and ii, of hBMSC do not give specific information about various organelles in the cell. We therefore performed six-level cluster analysis which resulted in five clusters for the cell and one for the background (magenta pixels), as shown in Figure 4C. Figure 4E shows the results of subtraction of the average background spectrum from each of the cluster spectra. The color coding in Figure 4E corresponds to the colors in the cluster image in Figure 4C. The black spectrum in Figure 4E shows a prominent band at 718  $\text{cm}^{-1}$  assigned to the C–N vibration in the phospholipid headgroup of the membrane lipid phosphatidylcholine (PC). Since PC is abundantly present in the plasma membrane of the cell as well as in the membranes of cell organelles,<sup>49</sup> the black cluster in Figure 4C can be assigned to the cell membrane and lipoproteins in the vicinity of it. The dark blue and light blue Raman spectra in Figure 4E show intense bands of nucleotides at 729, 750, 782, 895, 1091, and 1575  $\text{cm}^{-1}$  showing the presence of DNA distributed in the nucleus of the hBMSC. The spectral intensity of the light blue regions is higher than that of the dark blue region, which suggests that the DNA concentration is higher in the light blue regions than in the dark blue regions. The areas with high DNA content in the nucleus of the hBMSC are attributed to heterochromatin, and the regions of low DNA content are attributed to euchromatin. The green spectrum in Figure 4E shows bands at positions 718, 1076, 1260, 1298, 1437, and 1740  $\text{cm}^{-1}$  reflecting

(47) Chiang, H. K.; Peng, F.-Y.; Hung, S.-C.; Feng, Y.-C. *J. Raman Spectrosc.* **2009**, *40*, 546–549.

(48) Stewart, S.; Shea, D. A.; Tarnowski, C. P.; Morris, M. D.; Wang, D.; Franceschi, R.; Lin, D. L.; Keller, E. *J. Raman Spectrosc.* **2002**, *33*, 536–543.

(49) van Manen, H.-J.; Lenferink, A.; Otto, C. *Anal. Chem.* **2008**, *80*, 9576–9582.



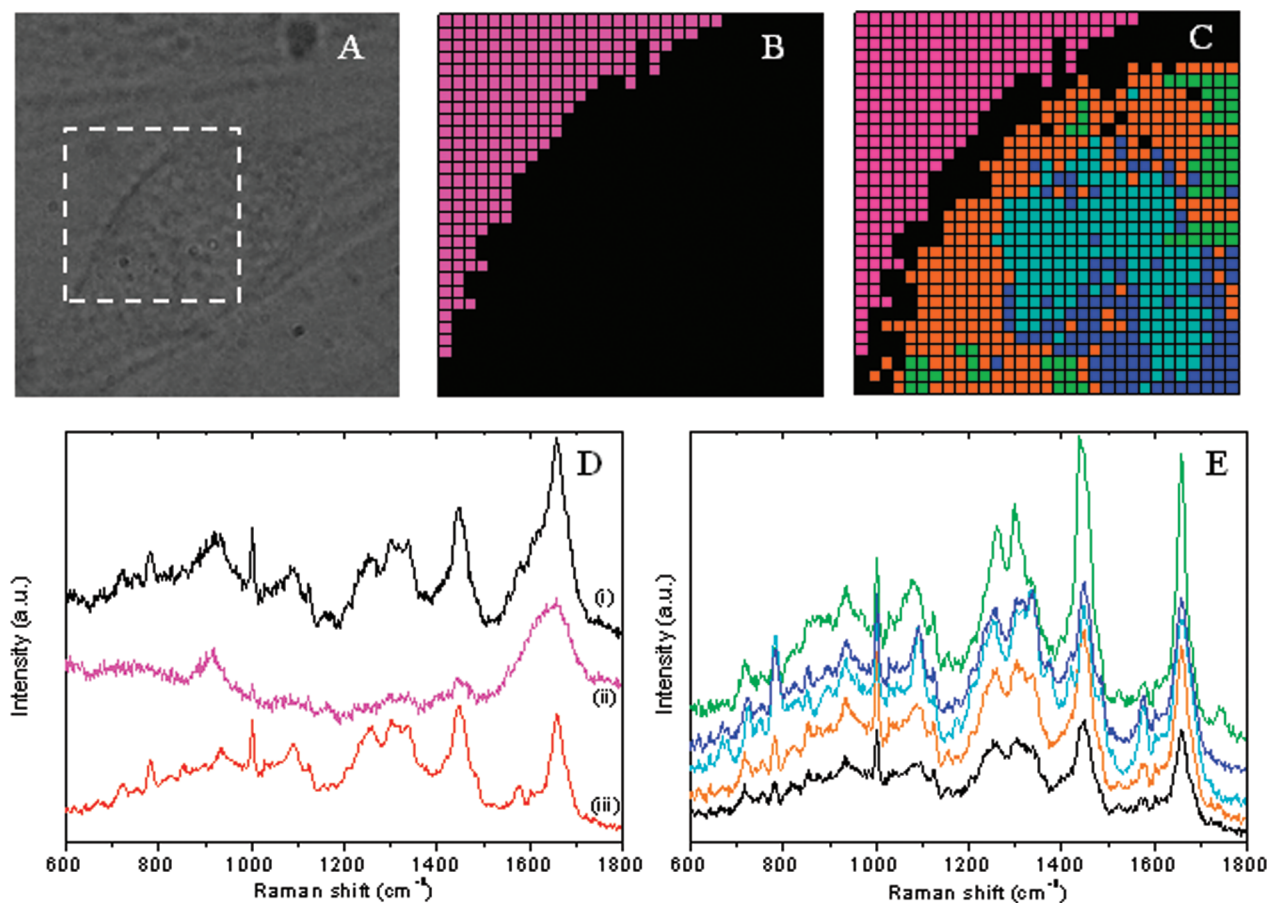


**Figure 4.** High spatial resolution Raman imaging performed on hBMSC cultured in  $\mu$ BR-II. hBMSCs were cultured under the influence of continuous perfusion of basic media up to day 4 of the culture period. (A) White-light micrograph showing hBMSC adhered to the glass coverslip. The white square box indicates the region of interest of  $15 \times 15 \mu\text{m}^2$  where Raman imaging is performed. (B) Two-cluster image of the obtained hyperspectral data (one cluster each for cell and background). (C) Six-cluster image of the hyperspectral data (five clusters for the cell and one cluster for background). (D) Corresponding average cell spectra of the two-cluster image over the spectral region of  $600\text{--}1800 \text{ cm}^{-1}$ : (i) average spectrum for the cell, (ii) average spectrum for the background, and (iii) Raman difference spectra of spectrum i minus spectrum ii showing the background-free cell spectrum. (E) Background-free spectra for the clusters corresponding to the cell in panel C over the spectral region of  $600\text{--}1800 \text{ cm}^{-1}$ . The color coding in panel E corresponds to that of the cluster image C. Raman imaging was performed over living hBMSC by scanning in  $32 \times 32$  steps over an area of  $15 \times 15 \mu\text{m}^2$  with an accumulation time of 0.5 s per pixel and 50 mW of laser power.

the presence of intracellular lipids. The clusters in Figure 4C corresponding to these spectra show the distribution of lipids in the region of interest over the hBMSC. The orange color spectrum in Figure 4E has bands corresponding to both proteins and lipids. The regions occupied by the corresponding pixels seen in Figure 4C can be attributed to the cytosol present in the cytoplasm of the cell. The spectrum of this cluster shows a small band at  $1602 \text{ cm}^{-1}$ , which can be attributed to mitochondria.<sup>50</sup> The spectrum also shows a band at  $718 \text{ cm}^{-1}$  for CN stretching vibration in phosphatidylcholine lipid headgroup, which is abundantly present in the mitochondrial membrane.<sup>50</sup> The average spectra in Figure 4E also show bands for amino acids, amides, and proteins present in the respective clusters.<sup>43–45</sup>

In conclusion, we have demonstrated the fabrication and use of microbioreactors for long-term perfusion culture of cells for as long as 21 days in  $\mu$ BR-I. The hBMSCs were successfully cultured inside the microchamber of the microbioreactors under continuous perfusion of the culture medium. The cells were kept in healthy condition throughout the culture period. The microbioreactors enabled optical Raman analysis of the cells cultured inside

the microbioreactor without disturbing the cells. Raman spectroscopy enabled noninvasive and label-free methodology to follow the differentiation and mineralization of the hBMSCs over a 21 day culture period in  $\mu$ BR-I. The results showed mineralization as early as day 14 of the culture period, and it increased in concentration by day 21. High spatial resolution Raman imaging of hBMSCs cultured in  $\mu$ BR-II showed the distribution of cell organelles in an individual hBMSC. These results show the feasibility of using confocal microspectroscopy for chemical imaging of differentiation of hBMSCs for tissue engineering in microbioreactors.

#### ACKNOWLEDGMENT

We thank the Dutch Program for Tissue Engineering for financial support (Grant No. TGT.6737).

#### SUPPORTING INFORMATION AVAILABLE

Additional information as noted in text. This material is available free of charge via the Internet at <http://pubs.acs.org>.

Received for review November 4, 2009. Accepted January 23, 2010.

AC902515C

(50) Pully, V. V.; Otto, C. J. *Raman Spectrosc.* **2009**, *40*, 473–475.